Enhanced transparency through second phase crystallization in BaAl$_4$O$_7$ scintillating ceramics

Marina Boyer[*,a], Salaheddine Alahraché[a], Cécile Genevois[a], Marina Licheron[a], François-Xavier Lefevre[b], Célia Castro [c], Guillaume Bonnefont[d], Gaël Patton[e], Federico Moretti[e], Christophe Dujardin[e], Guy Matzen[a] and Mathieu Allix[*,a]

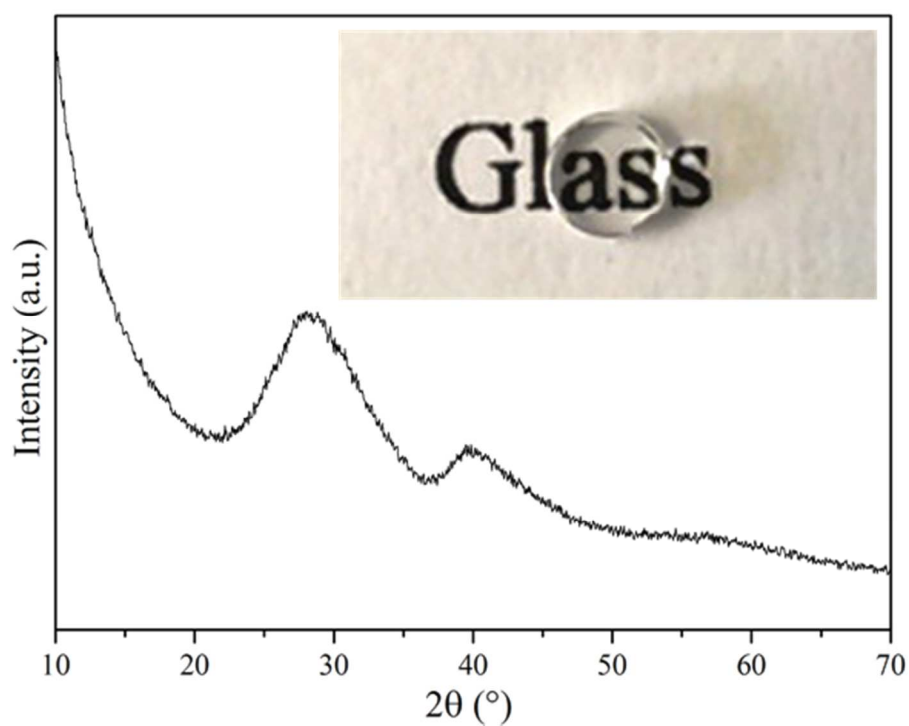**SUPPLEMENTARY INFORMATIONS**

Figure SI1: XRD pattern of the 35BaO-65Al$_2$O$_3$ glass confirming its amorphousness. The photography of the corresponding glass is in inset.
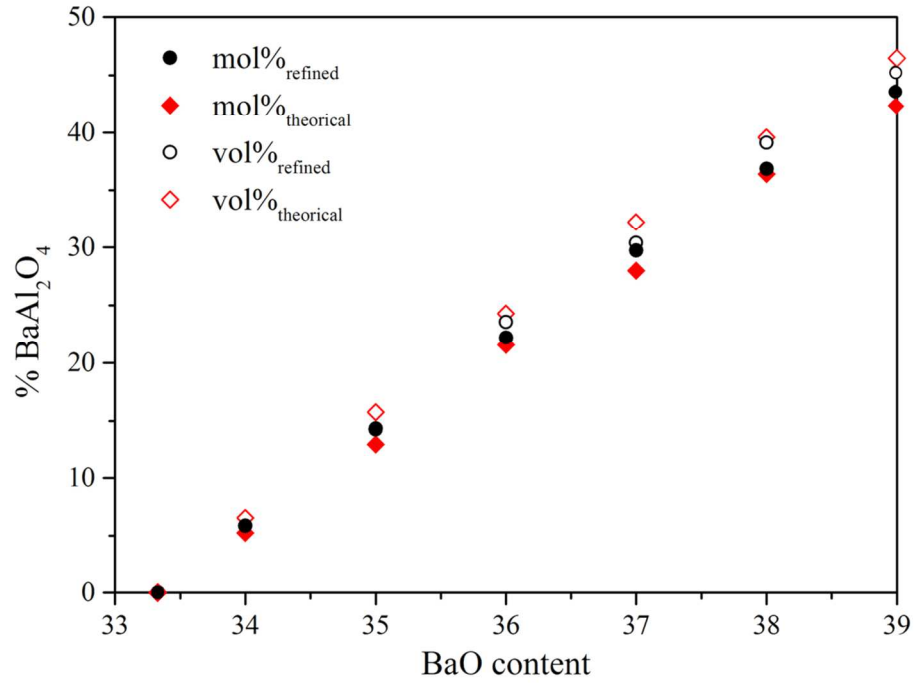
Figure SI2: Quantification of the $BaAl_2O_4$ contents in the studied biphasic $BaAl_4O_7$ - $BaAl_2O_4$ transparent polycrystalline ceramics. Both molar and volume fractions are represented. The values are obtained from Rietveld refinements performed on powder X-ray diffraction data and compared to the theoretical values deduced from nominal compositions.
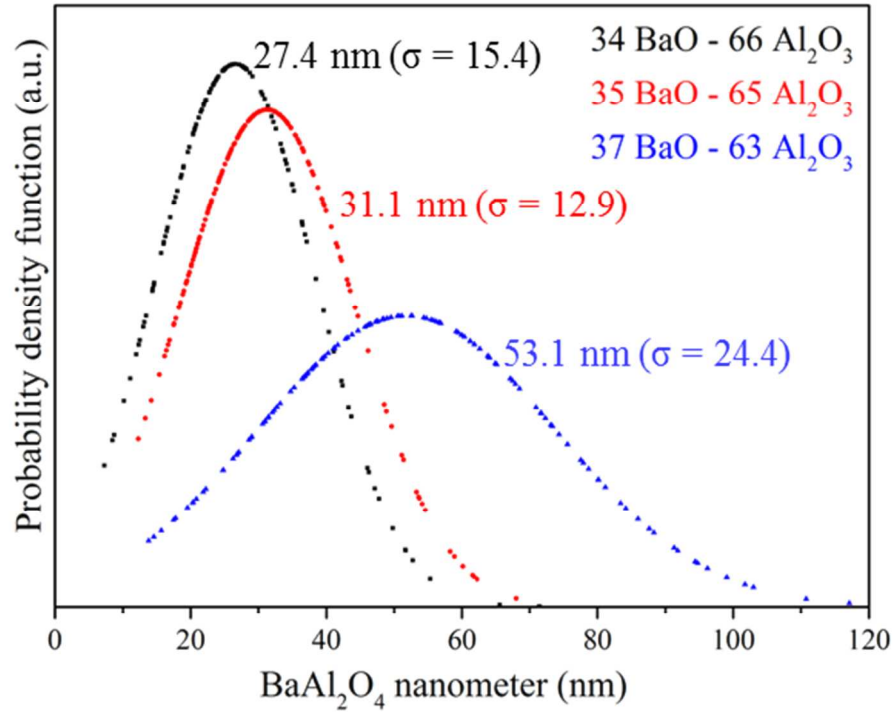

Figure SI3: Normal distribution of $BaAl_2O_4$ nanoparticles sizes, for the $34BaO$-$66Al_2O_3$, $35BaO$-$65Al_2O_3$, and $37BaO$-$63Al_2O_3$ polycrystalline ceramic compositions. The diameters were determined from TEM patterns.
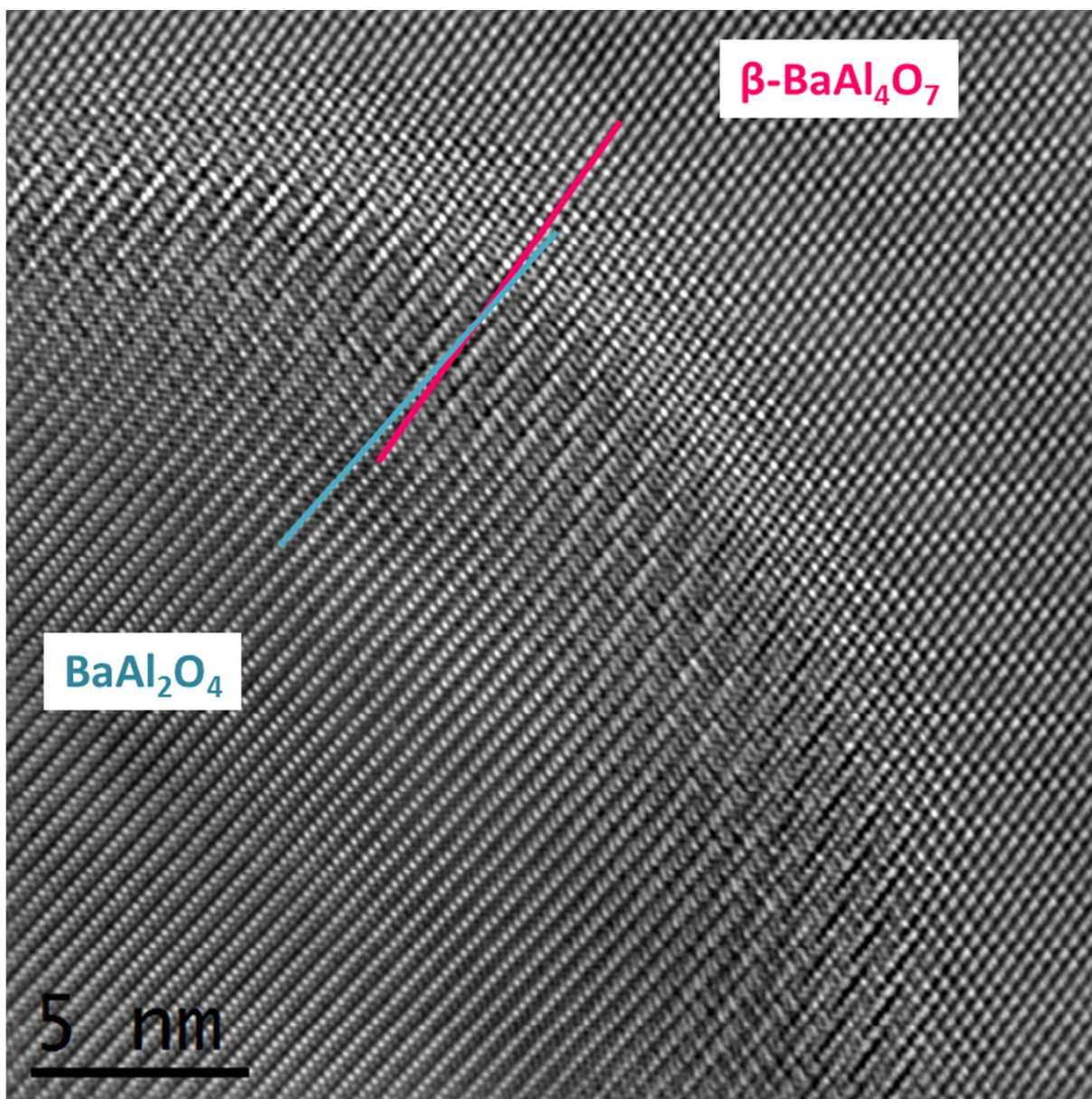
Figure SI4: Filtered HRTEM image of a $BaAl_2O_4$ nanoparticle into a $BaAl_4O_7$ grain, with a 6° misfit between the two crystallographic orientations.

$$n_x = -3.79 \times 10^{-12}\lambda^2 + 1.5866 + \frac{8934.6}{\lambda^2} + \frac{2.72 \times 10^8}{\lambda^4}$$

$$n_y = -2.97 \times 10^{-12}\lambda^2 + 1.5960 + \frac{8939.5}{\lambda^2} + \frac{2.46 \times 10^8}{\lambda^4}$$

$$n_z = -9.02 \times 10^{-12}\lambda^2 + 1.5871 + \frac{9090.2}{\lambda^2} + \frac{3.71 \times 10^8}{\lambda^4}.$$

Figure SI5: Expression of the refractive index components of β-BaAl$_4$O$_7$ along the three crystallographic orientations in the $500 - 4000$ nm range. These values were obtained from DFT calculations.[28]
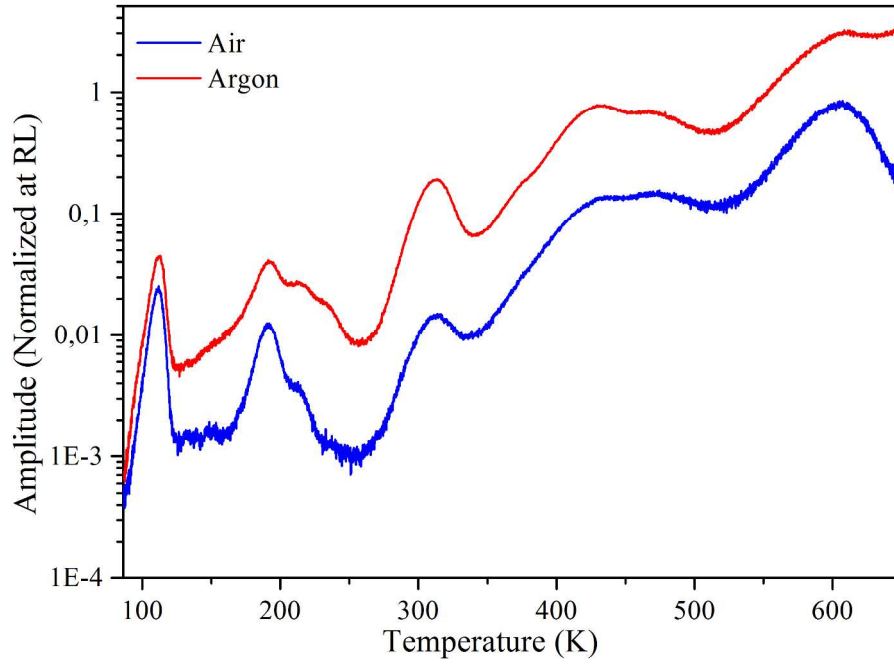

Figure SI6: Comparison of TSL from 90 to 670 K for the 34BaAl-66Al$_2$O$_3$ sample grown in air and in argon.